JOURNAL OF SPACECRAFT AND ROCKETS
Vol. 29, No. 3, May-June 1992

Buffet Response of a Hammerhead Launch Vehicle Wind-Tunnel Model

Stanley R. Cole*
NASA Langley Research Center, Hampton, Virginia 23665
and
Thomas L. Henning†
General Dynamics Space Systems Division, San Diego, California 92138

A wind-tunnel test of a 1/10th-scale Atlas-Centaur I launch vehicle model was conducted in the NASA Langley Transonic Dynamics Tunnel. The model was aeroelastically scaled to simulate flight bending modes using a partial mode technique. Several payload fairing configurations were tested at various angles of attack. No aeroelastic instabilities were found, and each configuration was generally more sensitive to Mach number variations than changes in angle of attack. Small length-to-diameter fairing ratios produced changes in buffet response in the second bending mode configuration. Additional testing was performed with vertical rods attached to the sting support to reduce the effects of mechanical vibration induced through the facility. The first flight of the Atlas-Centaur I vehicle successfully occurred on July 25, 1990, and the flight response was found to be well within the 3σ level of the wind-tunnel data.

Nomenclature

A = payload fairing cross-sectional (frontal) area, in.^{2}
B = peak bending moment, in.-lb
C_B = peak bending moment coefficient, B/qAD
C_σ = root-mean-square bending moment coefficient, σ/qAD
D = maximum payload fairing diameter, in.
f = frequency, Hz
H = length, in.
L = payload fairing cylindrical section length, in.
M = Mach number
m = generalized mass, slug
P = wind-tunnel drive power consumption, W
$\bar{P}$ = P normalized to P at $M = 1.2$
q = dynamic pressure, lb/in.^{2}
V = velocity, in./s
x = body station, in.
z = modal deflection normalized to maximum deflection
$\ddot{z}$ = vertical acceleration of sting support sector, g
$\bar{\ddot{z}}$ = $\ddot{z}$ normalized to $\ddot{z}$ at $M = 1.2$
α = angle of attack, deg
ρ = fluid density, lb-s^2/in.^{4}
σ = root-mean-square bending moment, in.-lb
ω = wind-tunnel drive rotational speed, Hz
$\bar{\omega}$ = ω normalized to ω at $M = 1.2$

Subscripts
i = ith vibration mode
v = full-scale vehicle
w = wind-tunnel model

Received Feb. 23, 1991; presented as Paper 91-1050 at the AIAA/ASME/ASCE/AHS/ASC 32nd Structures, Structural Dynamics, and Materials Conference, Baltimore, MD, April 8-10, 1991; revision received Dec. 20, 1991; accepted for publication Jan. 3, 1992.

*Aerospace Engineer, Configuration Aeroelasticity Branch, Structural Dynamics Division. Senior Member AIAA.
†Aerospace Engineer, Launch Vehicle Structural Dynamics.

Introduction

EVER increasing sizes and weights of launch vehicle payloads have resulted in an effort to provide a larger payload capability for the Atlas-Centaur launch vehicle (Fig. 1). The original Atlas-Centaur payload bay external diameter was the same as the propulsion stages of the launch vehicle. The new design, known as the Atlas-Centaur I Large Payload Fairing configuration (hereafter referred to as the Atlas-I LPF), has a 37.5% larger external diameter payload fairing. This new "hammerhead" payload fairing raised questions as to the unsteady aerodynamic loadings that might develop in flight. The NASA space vehicle design criteria specified in Ref. 1 would classify the Atlas-I LPF configuration as "buffet prone" compared with the baseline Atlas-Centaur that would be classified as a "clean body of revolution." Furthermore, wind-tunnel test results documented in Ref. 2 indicate a relationship between payload fairing cylinder length-to-diameter (L/D) ratios and vehicle stability. A Titan III hammerhead configuration with an $L/D = 0.4$ was shown to be unstable during that test. To correct this instability, the model L/D was increased to 1.1. A drawing of the eventual flight configuration of the Titan III concept is shown in Fig. 1 as the Titan-Centaur with an $L/D = 3.1$. Other launch vehicles are shown

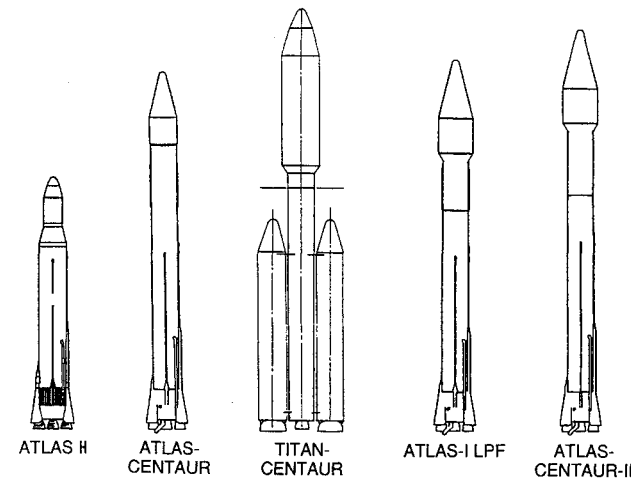

Fig. 1 Drawing of several launch vehicles.

in Fig. 1, such as the original Atlas-Centaur and the Atlas-I LPF, for comparison. The Atlas-I LPF configuration does not have the flow complexities associated with the large solid rocket motors of the Titan III configuration as shown in Fig. 1. However, the L/D ratio of the large payload fairing is 1.0. While the previous wind-tunnel test results do not provide sufficient data to define stability criteria for $0.4 < L/D < 1.1$, they do indicate potential stability problems for configurations in this range. These launch vehicle stability and buffet response phenomena are not easily predictable by analysis, although significant advances are being demonstrated through computational fluid dynamic techniques, such as documented in Ref. 3. Due to concerns about these phenomena, a wind-tunnel test was performed to determine such effects on the overall vehicle response of the Atlas-I LPF.

An aeroelastically scaled model of the Atlas-I LPF vehicle was constructed for wind-tunnel testing in the NASA Langley Transonic Dynamics Tunnel. The primary objectives of the wind-tunnel test were to verify that the Atlas-I LPF configuration was aeroelastically stable and to determine the overall vehicle bending moments due to buffet expected during transonic flight. A secondary objective was to conduct a parametric study to determine the effect of various hammerhead fairing configurations (in addition to the nominal design) on model response.

The purposes of this paper are to document general details of the model construction and to present some of the wind-tunnel test results. These results include the effects of various payload fairing configurations on the dynamic response of the model, interpretations of the response for the nominal flight configuration ($L/D = 1.0$), and an assessment of the influence of the sting mount system that was used for this test. Additionally, some full-scale vehicle results from the first flight of the Atlas-I LPF vehicle are presented and compared with wind-tunnel test results. The first flight of the Atlas-I LPF occurred on July 25, 1990.

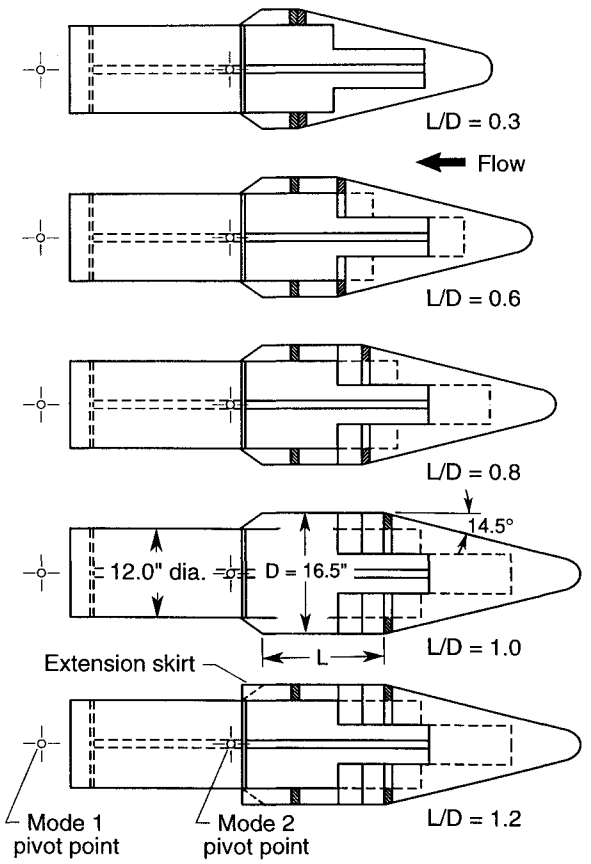

Fig. 2 Payload fairing configurations.

Wind Tunnel

The experimental study was conducted in the NASA Langley Transonic Dynamics Tunnel (TDT).[4] The TDT is specifically designed for studying aeroelastic phenomena. The facility is a continuous circuit wind tunnel capable of testing at total pressures from about 0.1 to 1.0 atm and over a Mach number range from 0 to 1.2. The test section of the TDT is 16.0 ft^2 with cropped corners. Testing can be conducted in the TDT using either air or a heavy gas as the test medium. The Atlas-I LPF model was aeroelastically scaled for and tested in the heavy gas. A unique safety feature of the TDT is a group of four bypass valves connecting the test section area (plenum) of the tunnel to the opposite leg of the wind-tunnel circuit. In the event of a model instability, such as severe buffeting, these quick-actuating values can be opened. This causes a rapid reduction in the test section Mach number and dynamic pressure. Operation of the bypass valves was never required for the model configurations tested. The combination of large-scale, high-speed, high-density, variable pressure, and the bypass valve system makes the TDT ideally suited for testing aeroelastically scaled models such as the Atlas-I LPF model.

Wind-Tunnel Model

The forebody model was scaled to the wind-tunnel size at an operating condition of $M = 0.9$ and $q = 300$ lb/ft^2 (2.083 lb/in.^{2}) by nondimensional length, time, and mass variables. The length was scaled based on blockage restrictions in the TDT to

$$\frac{H_w}{H_v} = 0.10$$

The frequency (time) relationship between wind-tunnel scale and full scale was derived from the Strouhal number equivalence

$$\left\{\frac{fH}{V}\right\}_w = \left\{\frac{fH}{V}\right\}_v$$

which leads to the relationship

$$\frac{f_w}{f_v} = \frac{H_v V_w}{H_w V_v} = 10\frac{V_w}{V_v} = 4.5$$

The mass of the wind-tunnel model was based on the nondimensional mass ratio defined as

$$\left\{\frac{m}{\rho H^3}\right\}_w = \left\{\frac{m}{\rho H^3}\right\}_v$$

which leads to the relationship

$$\frac{m_w}{m_v} = \frac{H_w^3 \rho_w}{H_v^3 \rho_v} = 0.001\frac{\rho_w}{\rho_v} = 0.00225$$

Damping was accounted for through measured model damping and estimates of flight vehicle damping. The model was constructed to provide a relatively small amount of structural damping to more closely match the full-scale vehicle damping.

The length and diameter dimensions of the payload fairing are indicated on the $L/D = 1.0$ configuration drawing of the Atlas-I LPF model body in Fig. 2. The $L/D = 1.0$ payload fairing configuration shown in Fig. 2 is the nominal design for the full-scale flight vehicle. For the parametric study of the effects of the payload fairing L/D ratio, model configurations were tested with L/D ratios of 0.3, 0.6, 0.8, 1.0, and 1.2. Drawings of these various configurations are also shown in Fig. 2.

More details on the construction of the Atlas-I LPF model are shown in Fig. 3. The payload fairing portion of the wind-tunnel model was constructed of foam-lined fiberglass forms. A cylindrical section of the payload fairing could be replaced

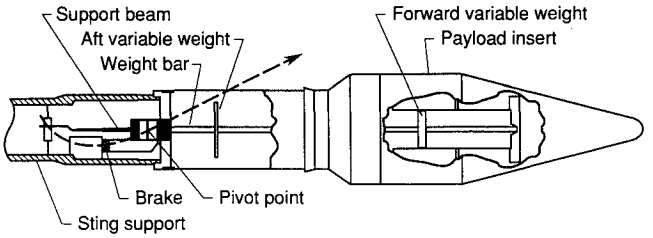

Fig. 3 Drawing showing model details.

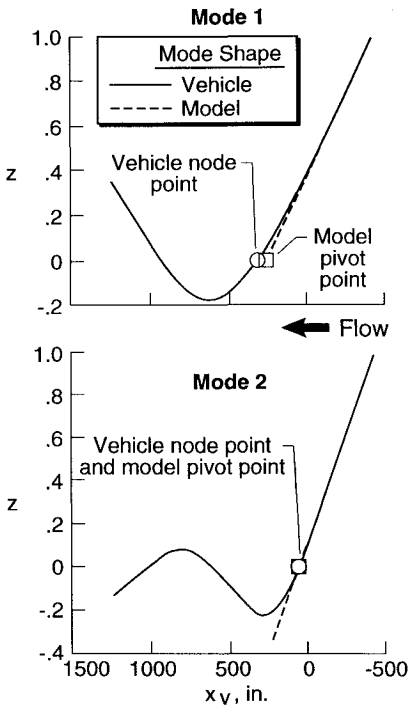

Fig. 4 Normalized vehicle mode shapes and linearized model mode shapes (scaled to flight) utilized for partial mode simulation.

with different length cylinders to vary the fairing ratio from $L/D = 0.3$ to 1.0. An extension skirt mounted at the aft end of the $L/D = 1.0$ payload fairing provided the $L/D = 1.2$ configuration. Variable weights were available in the payload fairing and in the model aft of the payload fairing (see Fig. 3) so that the total weight and weight distribution of the model could be adjusted with each L/D configuration to properly scale to the full-scale flight vehicle. Another special feature of the model was an internal hydraulic braking system (Fig. 3) that was intended to suppress excessive motion should the model experience severe buffeting or a divergent dynamic instability.

Partial Mode Simulation

The wind-tunnel model configurations were dynamically scaled to simulate either the first or second vehicle bending modes during transonic flight. This partial mode testing technique[5] was developed at the NASA Ames Research Center and was used in the Ames 14-ft Transonic Wind Tunnel. The primary assumptions for this simulation are that, for a typical launch vehicle, the mode shape forward of the first node point can be considered linear and that the majority of the unsteady aerodynamic forces are introduced through the forward portion of the vehicle. Thus, a forebody model can be used to simulate the important structural dynamic properties and the majority of the unsteady aerodynamics of the entire launch vehicle. Figure 4 shows calculated mode shapes for a forward portion of the full-scale Atlas-I LPF vehicle for the first two modes. The mode shapes forward of the first node point are seen to be nearly linear. The Atlas-I LPF model was constructed to geometrically model the forward portion of the flight vehicle with a single pivot point (see Fig. 3) about which to simulate the structural dynamics of a given vibration mode forward of the first node point. The wind-tunnel models represent the linear (rigid) portion of the mode shapes forward of the first node point. Based on the assumptions used in the partial mode testing technique concerning the unsteady dynamic loading, the generalized mass of the wind-tunnel model is scaled from the generalized mass of the entire flight vehicle. Provisions were made to allow the model to be moved relative to the dynamic pivot point (see Fig. 5) and to redistribute the internal weight so that the frequencies and generalized mass of the first or second bending mode could be appropriately simulated. Since the full-scale vehicle is essentially axisymmetric, the vibration modes were modeled as two-dimensional, vertical-bending modes. This was considered sufficient due to the similarity of the primary pitch (vertical) bending modes and the primary yaw (lateral) bending modes for the Atlas-I LPF vehicle.

Some difficulty was experienced in correctly modeling these two mode shapes in the wind tunnel due to sting support flexibility. Vertical stiffening rods were attached to the sting support to help this situation. Figure 6 shows the effect of the stiffening rods on the first bending mode shape. The mode shapes shown in Fig. 6 have been normalized to the maximum measured deflection. With the stiffening rods installed, the pivoting motion of the model occurred about a point much

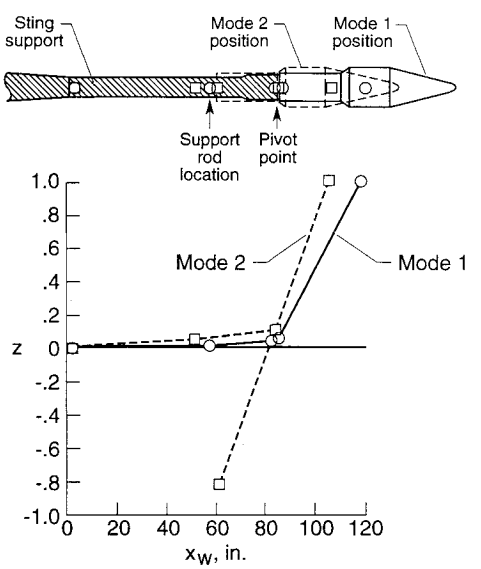

Fig. 5 Normalized mode shapes (with stiffening rods installed) and a drawing indicating position of payload fairing relative to pivot point for both mode simulations.

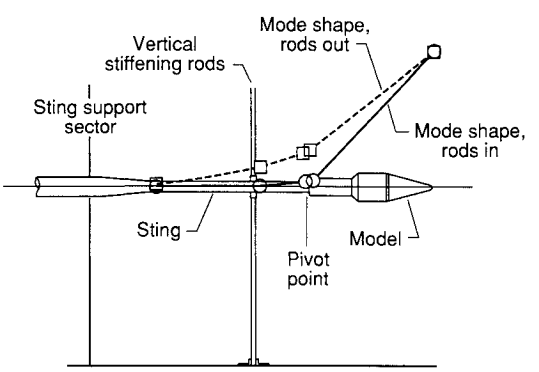

Fig. 6 Drawing of model with vertical stiffening rods installed showing the effect of the rods on the first bending mode shape (normalized).

closer to the intended rotation point than without the rods installed. This effect was much more pronounced in the first bending mode configuration due to the longer moment arm about which the model could rotate on the sting support system. Measurements showed that the vertical rods had little effect on model structural damping. Tests were conducted for both of the primary vibration modes with and without the vertical support rods installed in the tunnel. Although the rods-installed configuration is a slightly better representation of the flight vehicle, most of the testing was conducted for the second bending mode configuration without the rods installed to allow angle of attack variations of the model and to decouple the model from a closely spaced sting mode.

Vibration Characteristics

The structural dynamic properties of the 1/10th-scale Atlas-I LPF model were determined by ground vibration tests with the model mounted in the test section of the TDT. Vibration tests were conducted for the model in the first bending mode configuration and in the second bending mode configuration. The objectives of the vibration tests were to tune the model to the desired test frequency, to determine model mode shapes, and to obtain structural damping of the model for use in scaling of the test data to the full-scale vehicle values. The wind-tunnel model was tuned to $f_1 = 9.8$ Hz for the simulation of the first bending mode and to $f_2 = 25.0$ Hz for the second bending mode. Measured model normalized mode shapes for the simulation of the first two flight modes are shown in Fig. 5.

Instrumentation

The wind-tunnel model was instrumented with accelerometers and strain-gauge bridges for the buffet data acquisition. There were five biaxial accelerometers located in the model and on the model support sting. These accelerometers were capable of measuring vertical and lateral accelerations. Three of these five accelerometers were mounted within the model. The model was instrumented with two pitch bending moment strain-gauge bridges and with one yaw bending moment strain-gauge bridge near the pivot point.

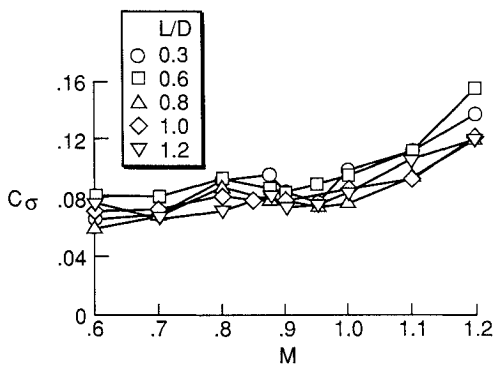

Fig. 7 Effect of L/D variations on buffet response for the first bending mode configuration without the vertical stiffening rods installed.

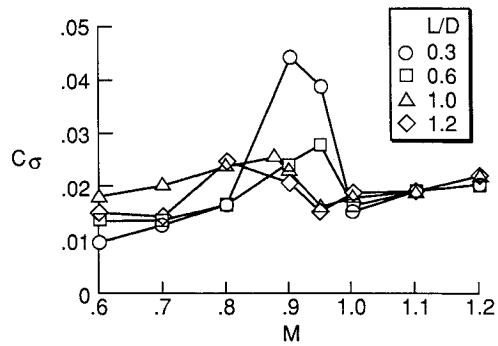

Fig. 8 Effect of L/D variations on buffet response for the second bending mode configuration without the vertical stiffening rods installed.

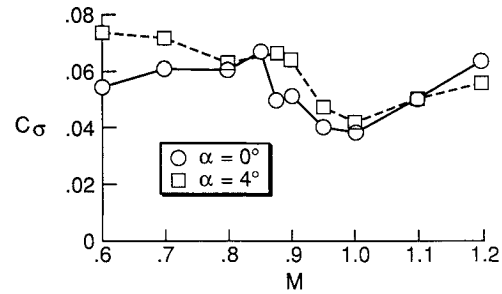

Fig. 9 Effects of M and α on σ measured at the pivot point for the first bending mode configuration with vertical stiffening rods installed ($L/D = 1.0$).

Results and Discussion

Wind-tunnel test results obtained using a 1/10th-scale Atlas-I LPF model have been used to verify the full-scale vehicle aeroelastic stability and to define induced bending moments. The $L/D = 1.0$ (rods-installed) configuration was the best available simulation of the flight vehicle and has shown that the flight vehicle will be free of dynamic instabilities and will experience acceptable buffet levels during flight. The scaled buffet loads found in the wind-tunnel test represent approximately 5–10% of the total vehicle design load, depending on the flight condition. In addition to flight clearance, some parametric studies were conducted during the wind-tunnel test. These studies include payload cylinder L/D variations and angle-of-attack variations for both of the primary vehicle bending modes that could be simulated by the model. The majority of these studies were conducted without the vertical rods installed to allow the angle of attack to be changed without entering the wind-tunnel test section. None of the configurations tested exhibited a dynamic instability.

L/D Variations

A number of configurations were tested to assess the effect of the L/D geometry parameter on the buffet response and dynamic stability of the Atlas-I LPF model. Figure 7 shows some of the acquired data for the first bending mode configuration without the vertical stiffening rods installed. The differences in the buffeting responses of the various L/D configurations of Fig. 7 are relatively small when considering the relationship of these data to the scaled design load capability of the flight vehicle. There is some indication that the lower L/D configurations induced greater buffet response, but the data are not entirely consistent concerning this trend. Before the test, it was expected that the model response would peak in the range of $0.80 \leq M \leq 0.95$ based on past experiences with launch vehicle unsteady loads. Figure 7 shows that the model exhibited a slight local peak in response near $M = 0.80$ for all of the L/D configurations except $L/D = 0.3$, which peaked closer to $M = 0.87$. But the wind-tunnel data further show that, after this slight peak, the response simply continues to grow with increasing Mach number. (Testing beyond $M = 1.2$ was not possible due to the operating capabilities of the TDT.) This response increase was not expected and is discussed further in the wind-tunnel influence subsection.

The response of the second bending mode configuration to L/D variations is shown in Fig. 8, again without the vertical stiffening rods installed. For the second bending mode, the response is found to peak in the Mach number range of $0.80 \leq M \leq 0.95$, but the response appears to be continuing to

increase with Mach number as the tunnel operating limits are reached at $M = 1.2$, as occurred with the first bending mode configuration. A subtle difference in the response due to the L/D variations is that there generally appears to be a slight increase (based on the Mach number trends of Fig. 8) in the Mach number at which the peak response occurs as the L/D is decreased. The $L/D = 0.3$ configuration of Fig. 8 (second mode) is the one configuration that shows a substantial increase in the dynamic response relative to the other L/D configurations. This may be an indication that the smallest L/D configuration tested was approaching a dynamic instability condition. Although the current state-of-the-art analysis techniques are unable to predict this type of phenomena, various mechanisms that can drive an aeroelastic instability have been proposed in Ref. 6. These mechanisms suggest that the added buffet effects of the large solid rocket motors on the Titan III wind-tunnel model may have contributed to the unstable response observed in that test (Ref. 2) as discussed in the introduction of this paper. The relationship, if any, of these possible mechanisms to the increased response found in this present study was not determined.

Angle-of-Attack Variations

Root-mean-square bending moment response measurements were made for $\alpha = 0.0$ and 4.0 deg for both of the Atlas-I LPF vibration mode configurations. Figure 9 shows typical root-mean-square bending moments as angle of attack and Mach number are varied for the $L/D = 1.0$ (rods-installed), first bending mode configuration. Figure 10 shows similar results for the $L/D = 1.0$, second bending mode configuration without the vertical stiffening rods installed. The first bending mode configuration is shown to be more sensitive to the angle-of-attack variation than the second bending mode configuration. For both modes, the model response was more dependent on Mach number variations than angle of attack for the range of conditions tested. Throughout this wind-tunnel test, the Mach number was varied continuously to evaluate the model response. Digital data, however, was only acquired at discrete Mach numbers.

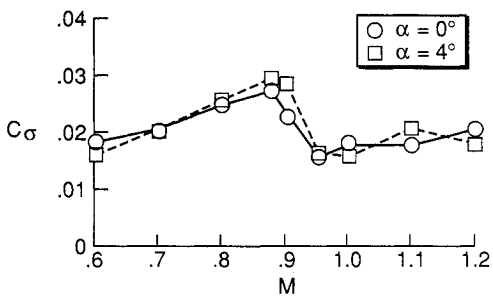

Fig. 10 Effects of M and α on σ measured at the pivot point for the second bending mode configuration with vertical stiffening rods installed ($L/D = 1.0$).

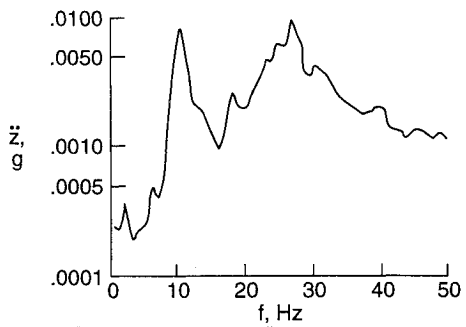

Fig. 11 Empty wind-tunnel frequency spectrum measured on the sting support sector ($M = 1.2$).

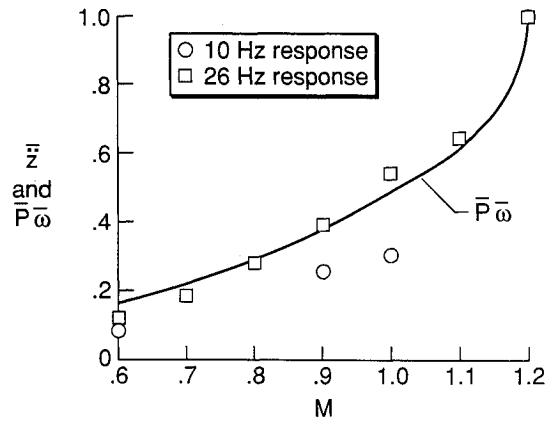

Fig. 12 Normalized support sector vertical response without model or sting mounted in wind tunnel.

Wind-Tunnel Influence

Because the response of the Atlas-I LPF model continued to increase above $M = 1.0$, some effort was made to assess the influence of the vibration levels associated with the wind-tunnel facility. Figure 11 shows measured vertical acceleration response of the wind-tunnel support sector without the model or sting installed. (The term "support sector" is used to describe the physical structure built into the TDT test section to support models mounted on a sting at the vertical centerline of the tunnel test section. The support sector in the TDT is constructed so that the model can be remotely pitched and traversed vertically in the test section.) The model was removed to eliminate its aerodynamic effect. The model alone would not be expected to have a significant dynamic influence on the measured sector response due to the massive nature of the support sector and the facility from which the forced response may have been emanating. Figure 11 seems to be consistent with the observations from oscillatory flow studies conducted in the TDT (using large flow vanes upstream of the test section to force oscillatory tunnel flow) that noted significant tunnel resonance effects above 10 Hz.[7,8] The frequency spectrum shown in this figure (for $M = 1.2$) clearly indicates two response peaks corresponding to approximately 10 and 26 Hz. These two frequencies are nearly the same values as those of the first bending and second bending mode configurations of the wind-tunnel model. Therefore, it is possible that the measured model response, although still at acceptable levels for the flight vehicle based on any of the model configurations, may actually be intensified by a wind-tunnel support sector forcing function at the same frequencies. Figure 12 shows normalized sting sector response as a function of Mach number. Some preliminary examination has indicated the possibility of a direct relationship between the wind-tunnel drive system total power consumption and fan rotational speed and the apparent sting support sector forcing function. Regardless of the source, Fig. 12 shows that the facility vibration continues to grow for any increase in Mach number with the rate of increase becoming even greater above $M = 1.0$. This suggests there may be a much stronger influence on the model response above $M = 1.0$. Since the buffet response of the wind-tunnel model was not severe for any of the configurations tested, the influence of the tunnel forcing response may have been great enough to somewhat hide the expected peak response in the transonic region as discussed in the preceding L/D variations subsection. Based on these test results, however, the buffet response data above $M = 1.0$ was not used to define vehicle design loads.

Figure 13 shows a comparison of the model responses of the $L/D = 1.0$ configuration for the support rods installed and not installed. These vertical stiffening rods would be expected to help reduce the influence of the facility forcing response through the sting support sector. The lower response of the rods-installed configuration suggests that the influence of the

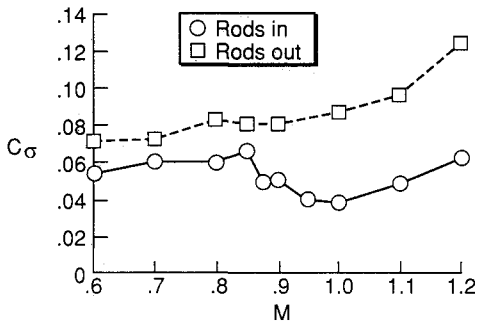

Fig. 13 Buffet response for the $L/D = 1.0$ payload fairing in the first bending mode configuration with and without the vertical stiffening rods installed.

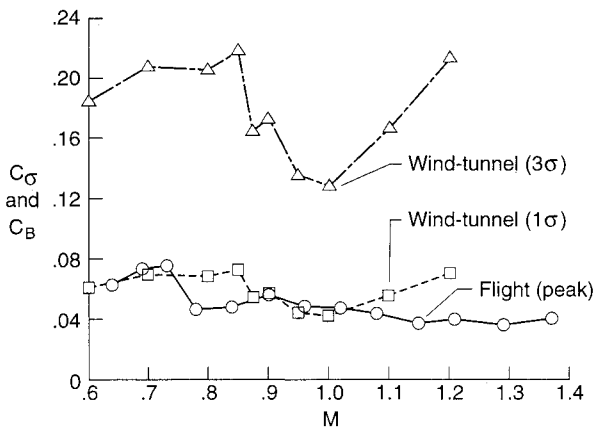

Fig. 14 Comparison of flight measurements with scaled wind-tunnel test measurements ($L/D = 1.0$, first bending mode configuration with vertical stiffening rods installed).

facility response is indeed less. Further, with the rods installed, the model exhibits a much more distinct transonic peak, although the model response still continues to increase beyond $M = 1.0$. The rods-installed configuration of Fig. 13 could perhaps be considered the best characterization of the model buffet response (least influenced by the facility), and the difference between the response of the rod-installed and the rods-not-installed configurations could be considered a portion of the measured response error due to the influence of the facility. Under these assumptions, the response error could be applied to the data of Fig. 7, and then each of the L/D configurations for the first bending mode model would exhibit a much more distinct transonic response peak.

Flight Vehicle Comparison

The first flight of the Atlas-I LPF vehicle successfully occurred on July 25, 1990. Some strain-gauge data were acquired from this initial flight that can be compared with results from the wind-tunnel test. This comparison is shown in Fig. 14. The wind-tunnel results are for the $L/D = 1.0$, first bending mode simulation configuration with the vertical stiffening rods installed. This configuration is considered to be the best available simulation of the flight vehicle. The coefficient C_σ shown for the wind-tunnel model in Fig. 14 has been scaled to full-scale flight data, including corrections for damping, and adjusted to represent the same body station as that measured in flight. Since the majority (greater than 95%) of the flight bending moment response at this station was found to be attributed to the first vehicle bending mode, it can be directly compared with the narrow-band response of the wind-tunnel model in the first bending mode configuration.

The first mode root-mean-square bending moments (σ) used in the calculation of C_σ for the wind-tunnel model were obtained based on relatively long time responses at constant tunnel conditions. Furthermore, through analysis of typical wind-tunnel data it was determined that the narrow-band frequency response near the first bending mode closely matches a probability density function[9] for a normal (Gaussian) random process. Based on these considerations, the probability that an instantaneous value of the bending moment will ever exceed 3σ is very small. This statistical information for the wind-tunnel model is useful in trying to assess the comparison with the flight data. The flight data shown in Fig. 14 represents peak values at rather rapidly changing Mach numbers during the vehicle atmospheric ascent. These peak-value bending moment coefficients cannot be compared with the wind-tunnel root-mean-square bending moments with any absolute certainty. Approximately 60 s of data were taken at any single Mach number during the wind-tunnel test compared with the full-scale vehicle passing through the peak response region ($0.75 < M < 0.90$) in approximately 6 s. Assuming that the flight data also approximate a normal random process, then it can be said that the flight data are well below the 3σ level determined by the wind-tunnel model, as would be expected. Although no proper conclusion can be drawn from this observation, it is interesting to note that the peak response flight data generally occurred near the 1σ level of the wind-tunnel model.

The flight data indicate a slight peak in the buffet response at approximately $M = 0.73$. The wind-tunnel data peaked at a higher Mach number condition, approximately $M = 0.85$. As previously discussed, the wind-tunnel model response continues to increase beyond $M = 1.0$, possibly due to the influence of wind-tunnel facility mechanical vibration. In comparison, the flight data tends to consistently decrease beyond $M = 1.0$ as was expected based on past experiences with launch vehicles.

Concluding Remarks

A wind-tunnel test of the Atlas-I Large Payload Fairing configuration was conducted in the Langley Transonic Dynamics Tunnel. A partial mode construction technique was used to aeroelastically scale the first two bending modes of the flight vehicle. The wind-tunnel results indicated that the flight vehicle would be free of dynamic instabilities and that the buffet loads would be less than 10% of the total vehicle design load at all flight conditions. In addition to the flight clearance studies, angle-of-attack and payload fairing L/D variations were tested.

The following statements summarize the most significant findings from the wind-tunnel test.

1) The buffet response level was not significantly affected by L/D variations except for the $L/D = 0.3$ fairing in the second bending mode configuration.

2) The variation in buffet response due to Mach number changes was of greater influence than that due to angle-of-attack changes.

3) The sting support sector vibration most likely increased the apparent buffet response. This effect appears to become even greater above $M = 1.0$. Vertical stiffening rods were installed on the sting support sector to help alleviate this effect.

4) Flight data show that the peak bending moments were well below the 3σ wind-tunnel data and level off above $M = 1.0$.

References

[1]Cole, H. A., Jr., Erickson, A. L., and Rainey, A. G., "Buffeting During Atmospheric Ascent," NASA SP-8001, 1963, revised Nov. 1970.

[2]Bombardier, G. D., "Final Post-Test Report on Seven Percent Transonic Buffet Model for Various Titan III Configurations," Martin Co., Rept. SSD-CR-66-563, Denver, CO, Jan. 1967.

[3]de Azevedo, J. L. F., "Transonic Aeroelastic Analysis of Launch Vehicle Configurations," NASA CR 4186, Oct. 1988.

[4]Reed, W. H., "Aeroelasticity Matters: Some Reflections of Two Decades of Testing in the NASA Langley Research Tunnel," NASA

TM-83120, Sept. 1981.

[5]Cole, H. A., Jr., "Dynamic Response of Hammerhead Launch Vehicles to Transonic Buffeting," NASA TN D-1982, July 1963.

[6]Ericsson, L. E., and Reding, J. P., "Fluid Dynamics of Unsteady Separated Flow, Part I, Bodies of Revolution," *Progress in Aerospace Science,* Vol. 23, No. 1, 1986, pp. 1–84.

[7]Mirick, P. H., Hamouda, M.-N. H., and Yeager, W. T., Jr., "Wind-Tunnel Survey of an Oscillating Flow Field for Application to Model Helicopter Rotor Testing," NASA TM 4224, Dec. 1990.

[8]Abbott, F. T., Jr., "Brief Description of the Characteristics of the Langley Transonic Dynamics Tunnel Airstream Oscillator," *Meeting on Aircraft Response to Turbulence,* NASA TM-82340, Sept. 1968, pp. 6.1–6.11.

[9]Curtis, A. J., "Concepts in Vibration Data Analysis," *Shock and Vibration Handbook,* edited by C. M. Harris and C. E. Crede, McGraw-Hill, New York, 1976, pp. 22-1–22-28.

Gerald T. Chrusciel
Associate Editor